Acta Medica
Okayama

*Original Article*

# Host-produced ADAMTS4 Inhibits Early-Stage Tumor Growth

Keiichi Asano[a,b], Midori Edamatsu[a], Omer F. Hatipoglu[b], Junko Inagaki[c],
Mitsuaki Ono[a], Takashi Ohtsuki[b], Toshitaka Oohashi[a], and Satoshi Hirohata[b]*

Departments of [a]Molecular Biology and Biochemistry and [c]Cell Chemistry,
Okayama University Graduate School of Medicine, Dentistry and Pharmaceutical Sciences,
[b]Department of Medical Technology, Graduate School of Health Sciences, Okayama University, Okayama 700-8558, Japan

Several research groups demonstrated that 'a disintegrin-like and metalloproteinase with thrombospondin type 1 motifs (ADAMTS)'-family proteases play roles in cancer progression. However, the origins and contributions of these proteases are not known. Here, we demonstrate an association between host-produced ADAMTS4 and early-stage tumor growth. Murine Lewis lung carcinoma (LLC) tumors showed marked expressions of *Adamts4* and *Adamts5*. We examined the contributions and distributions of host-derived *Adamts4* and *Adamts5* on tumor growth, using *Adamts4^(LacZ/LacZ)* and *Adamts5^(LacZ/LacZ)* knockout mice. Interestingly, the *Adamts4^(LacZ/LacZ)* mice showed enhanced tumor growth compared to wild-type mice at 5-, 10- and 12-days post-inoculation, whereas the *Adamts5^(LacZ/LacZ)* mice did not show significant differences in tumor growth. We next examined *LacZ* distribution in LLC tumor-bearing *Adamts4^(LacZ/LacZ)* mice by β-galactosidase (β-gal) staining. We found that the β-gal-positive signals were strictly localized at the interior areas of the tumor at 10 days post-inoculation. Multiple staining demonstrated that most of the β-gal-positive cells were localized at the tumor vasculature in *Adamts4^(LacZ/LacZ)* mice. Interestingly, β-gal-positive signals were not co-localized with biglycan after 10 days post-inoculation, excluding the biglycan cleavage by host-derived ADAMTS4. Taken together, these findings illustrate that host-derived ADAMTS4 was expressed at the tumor vessels and was associated with early-stage tumor growth.

Key words: ADAMTS, metalloproteinase, extracellular matrix, tumor microenvironment, mouse

Tumor tissues are comprised of tumor cells and stromal cells, including vascular cells, immune cells, and fibroblasts [1]. Crosstalk between tumor and non-tumor cells creates a specialized tumor microenvironment that determines the behavior of the tumor [2].

An abundant deposition of extracellular matrix (ECM), a major component of the tumor microenvironment, is associated with cancer progression. Since ECM remodeling is essential for multistep tumor growth, including invasion and metastasis, a number of studies have focused on matrix metalloproteinases (MMPs), a family of major ECM proteases [3]. 'A disintegrin-like and metalloproteinase with thrombospondin type 1 motif (ADAMTS)'-family proteases were identified as novel MMPs in a colon cancer cell line [4]. The 19 members of the ADAMTS family play roles in various diseases, including cancer [5-9]. Previous studies have demonstrated that, among the ADAMTS family members, ADAMTS4 and ADAMTS5 — both known as aggrecanases because they degrade aggrecan [10] — are dysregulated during cancer development [11,12]. Although ADAMTS4 and ADAMTS5 are well characterized as critical factors for osteoarthritis (as

aggrecanases promote the degradation of articular cartilage), the origins of ADAMTS4 and ADAMTS5 and their contributions to tumor progression are controversial [12-14]. We have sought to clarify the origins and contributions of host-derived ADAMTS4 and host-derived ADAMTS5 in tumor progression by developing and characterizing *Adamts4*<sup>LacZ/LacZ</sup> and *Adamts5*<sup>LacZ/LacZ</sup> knockout mice. Here, we demonstrate that deficiency in host-derived ADAMTS4, which was expressed in tumor vessels, resulted in altered tumor growth.

## Materials and Methods

***Mouse strains and cell culture.*** All animal experiments were approved by our institutional committee and adhered to the guidelines of Okayama University (#OKU-2017 175). *Adamts4*<sup>LacZ/LacZ</sup> and *Adamts5*<sup>LacZ/LacZ</sup> mice were purchased from The Jackson Laboratory (Bar Harbor, ME, USA) and maintained in a C57BL/6 background, as described [15,16]. C57BL/6 wild-type mice were purchased from Charles River Japan (Yokohama, Japan). Genomic DNA was extracted from mouse tails, using a DNeasy Blood & Tissue Kit (Qiagen, Hilden, Germany), and genotyping was performed using primer sets available at The Jackson Laboratory (Table 1). Cells of the murine Lewis lung carcinoma (LLC) cell line was purchased from the European Collection of Authenticated Cell Cultures (ECACC, Public Health England, Salisbury, UK). Cells were cultured in Dulbecco's modified Eagle's medium with 10% fetal bovine serum, 100 U/mL peni-

cillin and 100 μg/mL streptomycin in a 37°C humidified chamber (20% $O_2$ and 5% $CO_2$) [17]. All cells were maintained and used at passages 4-10.

***Tumor-bearing mouse model.*** LLC cells ($1.0 \times 10^6$) were inoculated in the skin of wild-type, *Adamts4*<sup>LacZ/LacZ</sup>, and *Adamts5*<sup>LacZ/LacZ</sup> mice (7-12 weeks old). Tumor volume was monitored every 2-3 days and calculated using the formula: volume = length × width$^2$ × 0.52, as described [18-20]. Tumor tissues were extracted either 10 days or 14 days after inoculation.

***RNA extraction and reverse transcription-polymerase chain reaction (RT-PCR).*** Total RNA was isolated from LLC-tumor tissues, using TRIzol reagent (Thermo Fisher Scientific, Waltham, MA, USA) [21,22], and RNA concentrations were determined using a NanoDrop™ spectrophotometer (Thermo Fisher Scientific). For the detection of *Adamts4* and *Adamts5* expression, reverse transcription-polymerase chain reaction (RT-PCR) was performed as described [23-26]. Briefly, 2 μg of RNA was reverse-transcribed with ReverTra Ace (Toyobo, Osaka, Japan), and cDNA was diluted fivefold with distilled water, as described [27,28]. The primers used for RT-PCR are shown in Table 2. The reactions involved 40 cycles at 60°C for *Adamts4* and *Adamts5* and 25 cycles at 63°C for *Actb*.

***β-galactosidase (β-gal) staining and immunohistochemistry.*** All tissues were fixed with 4% paraformaldehyde for 48 h at 4°C, incubated in 30% sucrose solution for 72 h at 4°C, and cryopreserved with O.C.T. compound (Sakura Finetek Japan, Tokyo, Japan) using liquid nitrogen. Tissues were sectioned to 5-10 μm by

**Table 1**    Primers used for genotyping

| Genes | Primer ID | Sequences |
|---|---|---|
| *Adamts4* Sense | moIMR0003 | 5'-GGG CCA GCT CAT TCC TCC CAC TCA T-3' |
| *Adamts4* Antisense #1 | oIMR4387 | 5'-GCA TAC CAC TCC AAA CTT AGA GAG G-3' |
| *Adamts4* Antisense #2 | oIMR4388 | 5'-CGC AGC TGA CTG CTC TTG TGC TTG-3' |
| *Adamts5* Sense | moIMR0012 | 5'-GGG TGG GAT TAG ATA AAT GCC TGC TCT-3' |
| *Adamts5* Antisense #1 | oIMR4996 | 5'-GGA CAC GGG ATG GAC CCT CTA GAT G-3' |
| *Adamts5* Antisense #2 | oIMR4997 | 5'-ACA TGG AGG ACT CAG TGT GGC CCA C-3' |

**Table 2**    Primers used for RT-PCR

| Genes | Sense primer | Antisense primer |
|---|---|---|
| *Adamts4* | 5'-CATCCTACGCCGGAAGAGTC-3' | 5'-AAGAGGCAGTGCCCATAACC-3' |
| *Adamts5* | 5'-CCTGCCCACCCAATGGTAAA-3' | 5'-GCAGCTGTGTAGAGTGTGGT-3' |
| *Actb* | 5 -TTCTACAATGAGCTGCGTGTGGC-3' | 5 -CTCATAGCTCTTCTCCAGGGAGGA-3' |

cryostat (Leica, Wetzlar, Germany). For β-gal staining, tissues were washed with wash buffer (0.1 M phosphate buffer pH 7.4, 2 mM $MgCl_2$, 0.01% Na deoxycholate, 0.02% NP-40) and then incubated with X-gal solution (0.1 M phosphate buffer pH 7.4, 2 mM $MgCl_2$, 0.01% sodium deoxycholate, 0.02% NP-40, 5 mM potassium ferrocyanide, 5 mM potassium ferricyanide, 2 mg/mL 5-bromo-4-chloro-3-indolyl β-D-galactopyranoside) at 37°C overnight [15].

The tissues were then washed with water three times for 5 min each and mounted. Counterstaining was performed with eosin. For immunostaining using peroxidase development, endogenous peroxidase was blocked with 0.3% $H_2O_2$ in methanol. Normal donkey serum (10%) was applied to block nonspecific binding of proteins. Tissues were incubated with primary antibody at 4°C overnight followed by secondary antibody for 1 h at room temperature.

The antibodies used in this study were: rat-anti-CD31 antibody (1 : 200, BD, Biosciences, San Jose, CA, USA); rat-anti-F4/80 antibody (1 : 100, MCA497GA, BioRad, Hercules, CA, USA); rabbit-anti-biglycan LF-159 (1 : 300, kindly provided by Drs. Larry W. Fisher and Marian F. Young, U.S. National Institutes of Health, Bethesda, MD, USA); biotinylated rabbit anti-rat IgG antibody (1 : 1000, BA-4001, Vector, Burlingame, CA, USA), biotinylated goat anti-rabbit IgG antibody (1 : 1000, BA-1000, Vector).

Tissues were treated with avidin-biotin complex (Vectastain Elite ABC kit, PK-6100, Vector) for 30 min. Immunostaining was developed using the DAB Substrate Kit (SK-4100, Vector) or AEC Substrate Kit (SK-4200, Vector), and sections were mounted as described [29-31]. Sections were imaged using a microscope (model BZ-X710, Keyence, Osaka, Japan) [32]. For multiple staining, immunostaining was performed after β-gal staining. For biglycan staining, tissues were incubated with 0.05 U/mL chondroitinase ABC (Sigma Aldrich, St. Louis, MO, USA; prepared in 0.03 M sodium acetate, 0.1 M Tris HCl, pH 8.0) for 1 h at 37°C.

***Statistical analysis.*** Values are presented as the mean ± standard deviation (SD). For multiple comparisons, an analysis of variance (ANOVA) was performed, followed by a post-hoc analysis with the Bonferroni test using SigmaPlot software. $P$-values < 0.05 were considered significant.

## Results

***Murine LLC expresses Adamts4 and Adamts5.*** As studies have suggested that several ADAMTS proteases, including ADAMTS4 and ADAMTS5, are dysregulated during cancer development, we first examined *Adamts4* and *Adamts5* expression in murine LLC-inoculated tumor tissues. The RT-PCR results demonstrated marked *Adamts4* and *Adamts5* expression in LLC tumor tissues (Fig. 1). Thus, we used this tumor model to investigate the origins and contributions of ADAMTS in tumor progression.

***Knockout of host Adamts4 but not Adamts5 significantly enhances tumor growth.*** To understand the contributions of host ADAMTS4 and ADAMTS5, we compared tumor growth in *Adamts4^{LacZ/LacZ}* and *Adamts5^{LacZ/LacZ}* mice with that in wild-type control mice. The knockout of *Adamts4* and *Adamts5* was confirmed by genotyping (Fig. 2). Interestingly, the LLC tumors grown in *Adamts4^{LacZ/LacZ}* mice, which lack host-derived *Adamts4*, had significantly increased volumes compared to those in the wild-type mice at 5 ($p < 0.05$), 10 ($p < 0.01$), and 12 ($p < 0.05$) days post-inoculation. However, the tumor volumes did not show significant differences at day 14 post-inoculation (Fig. 3A, B).

These results suggest the involvement of ADAMTS4 in early-stage tumor growth. In contrast, the tumors in the *Adamts5^{LacZ/LacZ}* mice did not show significant differences in volume compared to those in the wild-type mice. These results thus suggest that host ADAMTS4,
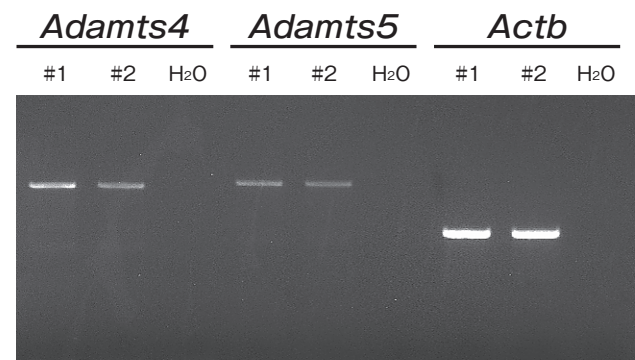


Fig. 1 *Adamts4* and *Adamts5* mRNA expression in Lewis lung carcinoma (LLC) tumors. RT-PCR of LLC-derived tumors was performed with *Adamts4* and *Adamts5* primer sets. A primer set for β-actin (*Actb*) was used as an internal control. PCR products were electrophoresed in 2.0% agarose gels, and the appropriately sized products were confirmed.
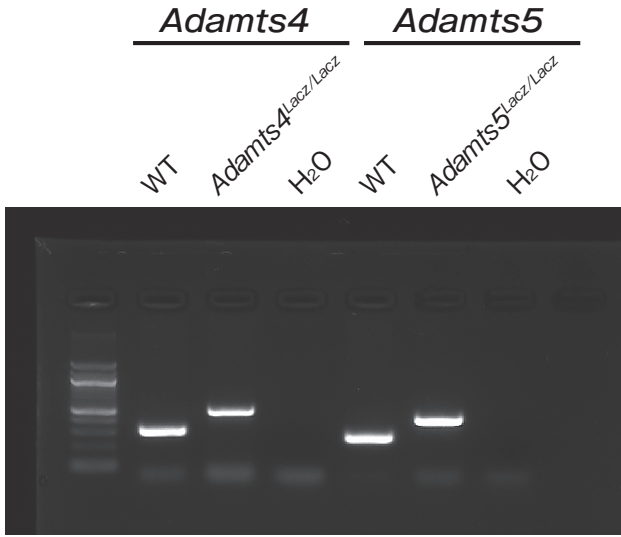
**Fig. 2**    Genotyping of *Adamts4*$^{LacZ/LacZ}$- and *Adamts5*$^{LacZ/LacZ}$-mice. Genomic DNA was extracted from wild-type, *Adamts4*$^{LacZ/LacZ}$, and *Adamts5*$^{LacZ/LacZ}$ mice. Genomic PCR was performed with specific primer sets for *Adamts4* and *Adamts5*. Amplified products were electrophoresed in 2.0% agarose gels, and amplicon sizes were confirmed.

but not ADAMTS5, has an inhibitory effect on early-stage tumor growth.

***LacZ gene expression in tumor development using Adamts4*** $^{LacZ/LacZ}$ ***and Adamts5*** $^{LacZ/LacZ}$ ***mice.***    To investigate the distribution of ADAMTS4 and ADAMTS5 in the tumor, we employed *LacZ* reporter gene systems in *Adamts4*$^{LacZ/LacZ}$ and *Adamts5*$^{LacZ/LacZ}$ mice, in which the *Adamts4* and *Adamts5* promoters regulate *LacZ* gene expression. We performed β-gal staining to visualize cells expressing *Adamts4* and *Adamts5*. We first validated the specificity of these systems in tissues known to express *Adamts4* and *Adamts5* (the adult eye for *Adamts4*; the adult kidney for *Adamts5*; Fig. 4A-D). We then examined β-gal positivity in the tumors of *Adamts4*$^{LacZ/LacZ}$ and *Adamts5*$^{LacZ/LacZ}$ mice. β-gal-positive signals were observed in the tumors in *Adamts4*$^{LacZ/LacZ}$ mice (Fig. 4E-G) at day 10 post-inoculation. The positive signals for β-gal staining at day 10 demonstrated limited distribution compared to those at day 14. That is, the β-gal staining was rather clear in the interior region of the tumor at 10 days post-inoculation, whereas the staining at day 14 was observed not only in the inte-
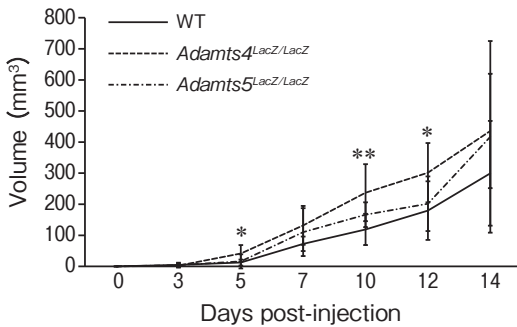


**Fig. 3**    Altered tumor growth in *Adamts4*-deficient mice. LLC cells were inoculated in the back skin of wild-type (WT), *Adamts4*$^{LacZ/LacZ}$, and *Adamts5*$^{LacZ/LacZ}$ mice (n = 8 for each group). **A**, Tumor growth in each group. *$p < 0.05$, **$p < 0.01$; **B**, All tumor volume data on days 5, 10, and 12 are plotted and compared. The median of the tumor volume is indicated. UD: undetectable. *$p < 0.05$, **$p < 0.01$, N.S., no significant difference.
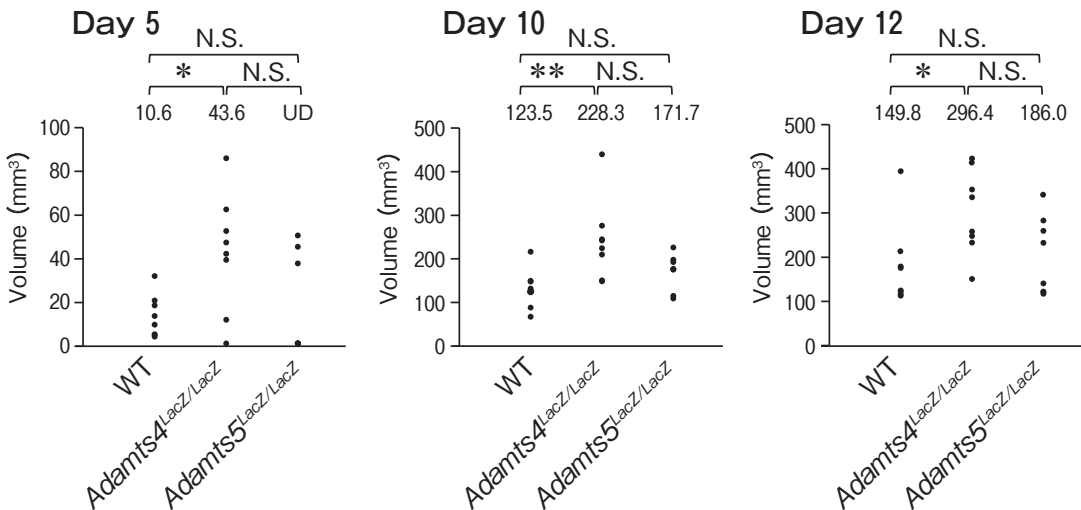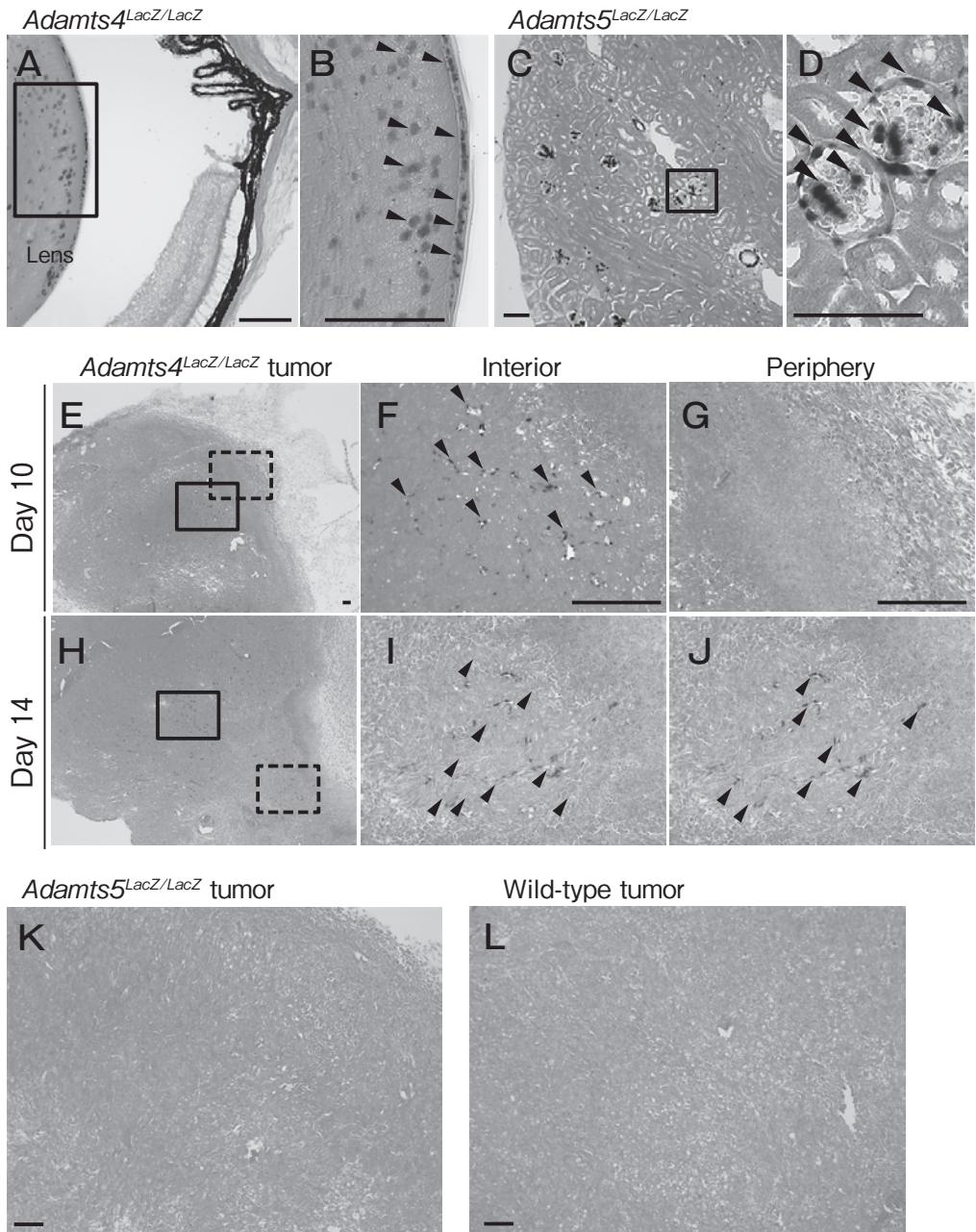
**Fig. 4** Histological analyses of host-derived *Adamts4* and *Adamt5* in the tumors. The expressions of host-derived *Adamts4* and *Adamts5* in the LLC tumors were analyzed by a *LacZ* reporter analysis. Each section was reacted with β-galactosidase (β-gal) in the appropriate conditions. Tissues were counterstained with eosin; **A**, β-gal activity in the eyes of *Adamts4^LacZ/LacZ^* mice served as a positive control; **B**, Higher magnification of the square region in (A). *Arrowheads*: β-gal activity in the lens; **C**, β-gal activity in the kidneys of *Adamts5^LacZ/LacZ^* mice was used as a positive control; **D**, Higher magnification of the square region in (C). *Arrowheads*: β-gal activity in the glomerulus; **E**, β-gal staining was performed on tumor sections from *Adamts4^LacZ/LacZ^* mice at day 10 after inoculation; **F**, Higher magnification of the solid square region in (E). *Arrowheads*: β-gal activity; **G**, Higher magnification of the dotted square region in (E). Note that β-gal activity was not observed in the periphery at this stage; **H**, Tumor sections from *Adamts4^LacZ/LacZ^* mice at day 14; **I**, Higher magnification of the solid square region in (H). *Arrowheads*: β-gal activity; **J**, Higher magnification of the dotted square region in (H). Note that β-gal activity was observed in the periphery as well at a later stage (*arrowheads*); **K**, β-gal staining was performed on tumor sections from *Adamts5^LacZ/LacZ^* mice; **L**, β-gal staining was performed on tumor sections from wild-type mice.

rior but also at the periphery of the tumors (Fig. 4H-J).

In contrast, the tumors in the *Adamts5^{LacZ/LacZ}* mice demonstrated little β-gal activity (Fig. 4K). Tumors in the wild-type mice served as a negative control, showing no β-gal activity (Fig. 4L). Therefore, host-derived ADAMTS4, but not host-derived ADAMTS5, was considerably expressed in the tumor tissues and showed a unique distribution change in the tumor development.

***Host ADAMTS4 localization at the tumor vascular endothelial cells.***   For the clarification of the role of ADAMTS4, it is important to identify which cells express ADAMTS4 in the tumor tissue. We thus next examined the co-staining of β-gal staining with an endothelial cell marker (CD31) and a macrophage marker (F4/80) in the *Adamts4^{LacZ/LacZ}* tumors. Interestingly, most of the β-gal-positive cells were co-stained with CD31 in the tumors at day 10, indicating that
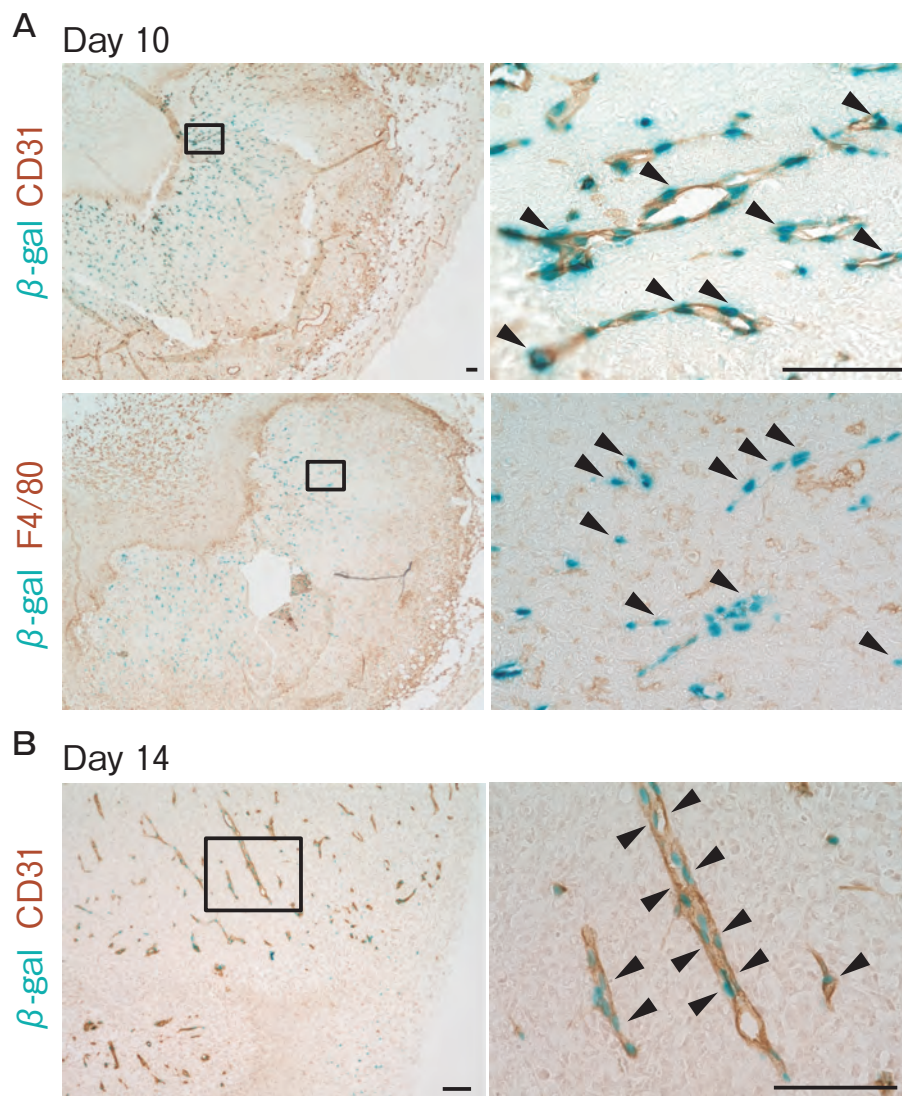


**Fig. 5**   *Adamts4* was distributed in the tumor vessels. **A**, CD31 immunostaining and F4/80 immunostaining (brown) was performed after β-gal staining (blue) using tumor sections from *Adamts4^{LacZ/LacZ}* mice at day 10 post-inoculation. Note that β-gal staining was observed mainly in the CD31-positive cells. *Arrowheads*: β-gal-positive cells; **B**, CD31 immunostaining was performed after β-gal staining using tumor sections from *Adamts4^{LacZ/LacZ}* mice at days 14. *Arrowheads*: β-gal activity (blue) in endothelial cells positive for CD31 (brown). Scale bar = 100μm.

*Adamts4* was expressed by endothelial cells on day 10 (Fig. 5A). In contrast, there was no clear co-staining between β-gal and F4/80 in the tumors at day 10 (Fig. 5A). Similarly, most of the β-gal-positive cells were CD31-positive in the tumors at 14 days post-inoculation (Fig. 5B). Thus, the majority of the *Adamts4*-expressing cells were endothelial cells.

***Biglycan distribution in tumor vascular endothelial cells.*** Because ADAMTS4 is a metalloproteinase, we next examined its substrate, biglycan, in the tumor tissue. Biglycan, a small leucine-rich repeat proteoglycan, was reported to be expressed in tumor vessels [33]. Biglycan and ADAMTS4 were reported to play a role in an *in vitro* angiogenesis model [34]. Here we performed serial section staining for β-gal staining and biglycan immunostaining. In the *Adamts4*$^{LacZ/LacZ}$ tumors at day 10, β-gal-positive cells were concentrated at interior areas (Fig. 6A-C), as also shown in Fig. 4.

Our immunostaining using an anti-biglycan antibody demonstrated limited biglycan distribution in the tumor periphery at 10 days after inoculation (Fig. 6D-F). In contrast, biglycan in the tumor 14 days after inoculation became more widely distributed in the tumor tissue (Fig. 6G, H). We also compared the localization of biglycan with β-gal activity in *Adamts4*$^{LacZ/LacZ}$ tumors and found that biglycan and β-gal signals were differently distributed at day 10, and biglycan co-localized with β-gal signals at day 14. Taken together, our find-
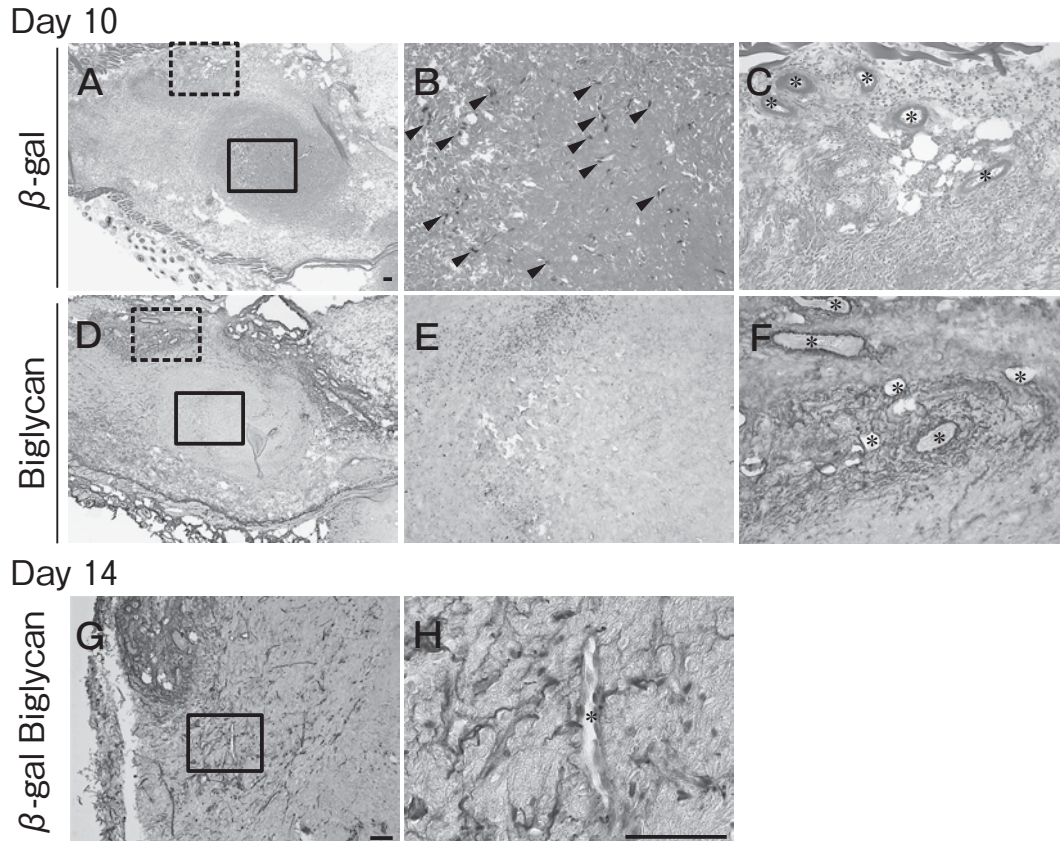


Fig. 6     Distribution of biglycan and *Adamts4* in the tumor tissue. **A**, β-gal staining in tumor sections from *Adamts4*$^{LacZ/LacZ}$ mice at day 10 post-inoculation. Interior and periphery regions of the tumor are shown; **B**, Higher magnification of the solid square region in (A). *Arrowheads*: β-gal-positive cells; **C**, Higher magnification of the dotted square region in (A). Note that no β-gal activity was observed at day 10. *The vessel cavit; **D**, Immunostaining for biglycan was performed using tumor serial sections from *Adamts4*$^{lacZ/lacZ}$ mice at day 10 post-inoculation; **E**, Higher magnification of the solid square region in (D); **F**, Higher magnification of the dotted square region in (D). Note that biglycan was distributed in the tumor periphery at day 10. *The vessel cavity; **G**, Immunostaining for biglycan was performed after β-gal staining in tumor sections from *Adamts4*$^{LacZ/LacZ}$ mice at day 14. Biglycan was localized at vessel-like structures positive for β-gal activity; **H**, Higher magnification of the square region in (G). *The vessel cavity. Scale bar = 100 μm.

ings suggest that (1) tumor vessel endothelial cells (*i.e.*, the host origin) express ADAMTS4, and (2) biglycan cleavage is not involved in the early stage (*i.e.*, day 10) of tumor growth.

## Discussion

Our study identified that host-derived ADAMTS4, not ADAMTS5, was expressed in the tumor vessels, and a lack of ADAMTS4 enhanced early-stage tumor growth. Although both ADAMTS4 and ADAMTS5 have been implicated in cancer, the details have not been elucidated. Our study is the first to report that host-derived ADAMTS4, but not host-derived ADAMTS5, plays a role in tumor growth.

We performed β-gal staining to determine *LacZ* expression, which replaced the *Adamts4* or *Adamts5* gene in the knockout mice. This analysis is advantageous because it does not require a target molecule-specific antibody [15]. In addition, this method can distinguish host-derived target molecules' distribution from that of tumor cell-derived target molecules with high sensitivity and high specificity in tumor-bearing mouse models. Because the tumor microenvironment is comprised of various cell types, including tumor cells and mesenchymal cells, it can be difficult to determine the localization of host-derived molecules in the tumor tissue. This analysis enabled the identification of the precise localization of host *Adamts4* and *Adamts5*. *LacZ* was markedly localized to endothelial cells in the tumors, indicating the distribution of host-derived *Adamts4* in our model. From this point of view, this method is superior to immunohistochemistry.

Many studies have reported that metalloproteinases are produced by tumor cells and play fundamental roles in tumor dissemination [3]. ADAMTS4 is expressed in many types of cancers [35,36]. Rao *et al.* reported that ADAMTS4 and its proteolytic fragments differentially affect tumor growth [13]. They used an ADAMTS4-transfected tumor cell implantation model and demonstrated that full-length ADAMTS4 promotes tumor growth and angiogenesis, whereas the C-terminal region of ADAMTS4 inhibits tumor growth.

Fernández-Rodríguez *et al.* reported that stroma-derived ADAMTS1 plays a role in tumor growth [37]. There is no report demonstrating the relevance of host-derived ADAMTS4 and ADAMTS5; we therefore decided to examine the effect of host-derived

ADAMTS4 and ADAMTS5 using *Adamts4^{LacZ/LacZ}* mice and *Adamts5^{LacZ/LacZ}* mice. We did not elucidate the effect of ADAMTS4 cleavage in our system, as we focused on the role of ADAMTS4 produced by host cells.

What is the role of host-derived ADAMTS4 in tumor growth? One possible answer is that it acts as a metalloprotease in the tumor vessels. Since ADAMTS4 is a major protease that degrades proteoglycans, it is thought to contribute to the clearance and remodeling of proteoglycans. Interestingly, previous investigations have demonstrated that biglycan, a chondroitin sulfate or dermatan sulfate proteoglycan, is a major substrate of ADAMTS4 [38] and that both biglycan and ADAMTS4 are associated with angiogenesis. We thus compared the histological distribution of biglycan by immunohistochemistry with that of *Adamts4* by β-gal staining. Interestingly, biglycan and β-gal staining demonstrated different distributions at the early stage (day 10) of tumor growth. This result indicated that biglycan is not likely to be a substrate in the tumor vessels at the early stage.

Our results may indicate an unknown substrate of ADAMTS4 at the early stage of tumor growth, including ADAMTS4 cleavage itself. On the other hand, we observed considerable biglycan accumulation in tumor vessels at the later stage (day 14), and these vessels were positive for β-gal in the *Adamts4^{LacZ/LacZ}* tumors. Interestingly, we observed that the proteoglycan versican, another possible substrate of ADAMTS4, also accumulates in the vasculature (Asano *et al.*, data in submission). These data may suggest a role of host-derived ADAMTS4 at the later stage of tumor development.

There are several ADAMTS family members that share high homology with ADAMTS4. ADAMTS5 was reported to play a role in tumor angiogenesis by down-regulating VEGF expression [39]. Kumar *et al.* reported that ADAMTS5 functions as an anti-angiogenic and anti-tumorigenic protein [40]. In our experimental model, the tumor growth in the *Adamts5^{LacZ/LacZ}* mice was not significantly different from that of the wild-type mice. Because β-gal activity was not detected in the tumor tissue in the *Adamts5^{LacZ/LacZ}* mice, we think that the host cells were not primarily expressing ADAMTS5, resulting in the lack of a significant difference in the tumor growth.

Our findings demonstrated that the tumor growth in the *Adamts4^{LacZ/LacZ}* mice was significantly different at early stages but not at the later stage. This may suggest

cooperative roles for multiple ADAMTS members at later stages of tumor growth, while ADAMTS4 is important for early-stage growth. Detailed analyses of the early stages of tumor development in *Adamts4*[*LacZ/LacZ*] mice and analyses using combinational ADAMTS knockout mice may provide additional information regarding the functions of ADAMTS4 in tumor growth.

In conclusion, our findings suggest that host-derived ADAMTS4, but not ADAMTS5, plays a role in early-stage tumor growth. Our study sheds light on the possible roles of host cells in the tumor microenvironment. The relationship between tumor-derived and host-derived ADAMTS4 will be clarified in future research.

# References

1. Quail DF and Joyce JA: Microenvironmental regulation of tumor progression and metastasis. Nat Med (2013) 19: 1423–1437.

2. Gadea BB and Joyce JA: Tumour-host interactions: implications for developing anti-cancer therapies. Expert Rev Mol Med (2006) 8: 1–32.

3. Kessenbrock K, Plaks V and Werb Z: Matrix Metalloproteinases: Regulators of the Tumor Microenvironment. Cell (2010) 141: 52–67.

4. Kuno K, Kanada N, Nakashima E, Fujiki F, Ichimura F and Matsushima K: Molecular Cloning of a Gene Encoding a New Type of Metalloproteinase-disintegrin Family Protein with Thrombospondin Motifs as an Inflammation Associated Gene. J Biol Chem (1997) 272: 556–562.

5. Nakamura K, Hirohata S, Murakami T, Miyoshi T, Demircan K, Oohashi T, Ogawa H, Koten K, Toeda K, Kusachi S, Ninomiya Y and Shiratori Y: Dynamic induction of ADAMTS1 gene in the early phase of acute myocardial infarction. J Biochem (2004) 136: 439–446.

6. Demircan K, Hirohata S, Nishida K, Hatipoglu OF, Oohashi T, Yonezawa T, Apte SS and Ninomiya Y: ADAMTS-9 is synergistically induced by interleukin-1beta and tumor necrosis factor alpha in OUMS-27 chondrosarcoma cells and in human chondrocytes. Arthritis Rheum (2005) 52: 1451–1460.

7. Demircan K, Gunduz E, Gunduz M, Beder LB, Hirohata S, Nagatsuka H, Cengiz B, Cilek MZ, Yamanaka N, Shimizu K and Ninomiya Y: Increased mRNA expression of ADAMTS metalloproteinases in metastatic foci of head and neck cancer. Head Neck (2009) 31: 793–801.

8. Hatipoglu OF, Hirohata S, Cilek MZ, Ogawa H, Miyoshi T, Obika M, Demircan K, Shinohata R, Kusachi S and Ninomiya Y: ADAMTS1 Is a Unique Hypoxic Early Response Gene Expressed by Endothelial Cells. J Biol Chem (2009) 284: 16325–16333.

9. Demircan K, Yonezawa T, Takigawa T, Topcu V, Erdogan S, Ucar F, Armutcu F, Yigitoglu MRR, Ninomiya Y and Hirohata S: ADAMTS1, ADAMTS5, ADAMTS9 and aggrecanase-generated proteoglycan fragments are induced following spinal cord injury in mouse. Neurosci Lett (2013) 544: 25–30.

10. Tortorella MD, Malfait A-M, Deccico C and Arner E: The role of ADAM-TS4 (aggrecanase-1) and ADAM-TS5 (aggrecanase-2) in a model of cartilage degradation. Osteoarthr Cartil (2001) 9: 539–552.

11. Binder MJ, McCoombe S, Williams ED, McCulloch DR and Ward AC: The extracellular matrix in cancer progression: Role of hyalectan proteoglycans and ADAMTS enzymes. Cancer Lett (2017) 385: 55–64.

12. Porter S: Dysregulated Expression of Adamalysin-Thrombospondin Genes in Human Breast Carcinoma. Clin Cancer Res (2004) 10: 2429–2440.

13. Rao N, Ke Z, Liu H, Ho C-J, Kumar S, Xiang W, Zhu Y and Ge R: ADAMTS4 and its proteolytic fragments differentially affect melanoma growth and angiogenesis in mice. Int J Cancer (2013) 133: 294–306.

14. Held-Feindt J, Paredes EB, Blömer U, Seidenbecher C, Stark AM, Mehdorn HM and Mentlein R: Matrix-degrading proteases ADAMTS4 and ADAMTS5 (disintegrins and metalloproteinases with thrombospondin motifs 4 and 5) are expressed in human glioblastomas. Int J Cancer (2006) 118: 55–61.

15. McCulloch DR, Goff C Le, Bhatt S, Dixon LJ, Sandy JD and Apte SS: Adamts5, the gene encoding a proteoglycan-degrading metalloprotease, is expressed by specific cell lineages during mouse embryonic development and in adult tissues. Gene Expr Patterns (2009) 9: 314–323.

16. Kumar S, Chen M, Li Y, Wong FHS, Thiam CW, Hossain MZ, Poh KK, Hirohata S, Ogawa H, Angeli V and Ge R: Loss of ADAMTS4 reduces high fat diet-induced atherosclerosis and enhances plaque stability in ApoE−/− mice. Sci Rep (2016) 6: 31130.

17. Ishii H, Kamikawa S, Hirohata S, Mizutani A, Abe K, Seno M, Oohashi T and Ninomiya Y: Eosinophil Cationic Protein Shows Survival Effect on H9c2 Cardiac Myoblast Cells with Enhanced Phosphorylation of ERK and Akt/GSK-3$\beta$ under Oxidative Stress. Acta Med Okayama (2015) 69: 145–153.

18. Miyoshi T, Hirohata S, Ogawa H, Doi M, Obika M, Yonezawa T, Sado Y, Kusachi S, Kyo S, Kondo S, Shiratori Y, Hudson BG and Ninomiya Y: Tumor-specific expression of the RGD-alpha3(IV) NC1 domain suppresses endothelial tube formation and tumor growth in mice. FASEB J (2006) 20: 1904–1906.

19. Obika M, Ogawa H, Takahashi K, Li J, Hatipoglu OF, Cilek MZ, Miyoshi T, Inagaki J, Ohtsuki T, Kusachi S, Ninomiya Y and Hirohata S: Tumor growth inhibitory effect of ADAMTS1 is accompanied by the inhibition of tumor angiogenesis. Cancer Sci (2012) 103: 1889–1897.

20. Hofmann M, Pflanzer R, Zoller NN, Bernd A, Kaufmann R, Thaci D, Bereiter-Hahn J, Hirohata S and Kippenberger S: Vascular endothelial growth factor C-induced lymphangiogenesis decreases tumor interstitial fluid pressure and tumor. Transl Oncol (2013) 6: 398–404.

21. Yaykasli KO, Oohashi T, Hirohata S, Hatipoglu OF, Inagawa K, Demircan K and Ninomiya Y: ADAMTS9 activation by interleukin 1 beta via NFATc1 in OUMS-27 chondrosarcoma cells and in

human chondrocytes. Mol Cell Biochem (2009) 323: 69–79.

22. Hatipoglu OF, Hirohata S, Yaykasli KO, Cilek MZ, Demircan K, Shinohata R, Yonezawa T, Oohashi T, Kusachi S and Ninomiya Y: The 3'-untranslated region of ADAMTS1 regulates its mRNA stability. Acta Med Okayama (2009) 63: 79–85.

23. Inagaki J, Takahashi K, Ogawa H, Asano K, Faruk Hatipoglu O, Zeynel Cilek M, Obika M, Ohtsuki T, Hofmann M, Kusachi S, Ninomiya Y and Hirohata S: ADAMTS1 inhibits lymphangiogenesis by attenuating phosphorylation of the lymphatic endothelial cell-specific VEGF receptor. Exp Cell Res (2014) 323: 263–275.

24. Shen Z-N, Nishida K, Doi H, Oohashi T, Hirohata S, Ozaki T, Yoshida A, Ninomiya Y and Inoue H: Suppression of chondrosarcoma cells by 15-deoxy-Delta 12, 14-prostaglandin J2 is associated with altered expression of Bax/Bcl-xL and p21. Biochem Biophys Res Commun (2005) 328: 375–382.

25. Komata T, Koga S, Hirohata S, Takakura M, Germano I, Inoue M, Kyo S, Kondo S and Kondo Y: A novel treatment of human malignant gliomas in vitro and in vivo: FADD gene transfer under the control of the human telomerase reverse transcriptase gene promoter. Int J Oncol (2001) 19: 1015–1020.

26. Takemoto S, Murakami T, Kusachi S, Iwabu A, Hirohata S, Nakamura K, Sezaki S, Havashi J, Suezawa C, Ninomiya Y and Tsuji T: Increased expression of dermatopontin mRNA in the infarct zone of experimentally induced myocardial infarction in rats: comparison with decorin and type I collagen mRNAs. Basic Res Cardiol (2002) 97: 461–468.

27. Toeda K, Nakamura K, Hirohata S, Hatipoglu OF, Demircan K, Yamawaki H, Ogawa H, Kusachi S, Shiratori Y and Ninomiya Y: Versican is induced in infiltrating monocytes in myocardial infarction. Mol Cell Biochem (2005) 280: 47–56.

28. Yamawaki H, Hirohata S, Miyoshi T, Takahashi K, Ogawa H, Shinohata R, Demircan K, Kusachi S, Yamamoto K and Ninomiya Y: Hyaluronan receptors involved in cytokine induction in monocytes. Glycobiology (2009) 19: 83–92.

29. Sezaki S, Hirohata S, Iwabu A, Nakamura K, Toeda K, Miyoshi T, Yamawaki H, Demircan K, Kusachi S, Shiratori Y and Ninomiya Y: Thrombospondin-1 is induced in rat myocardial infarction and its induction is accelerated by ischemia/reperfusion. Exp Biol Med (Maywood) (2005) 230: 621–630.

30. Nasu Y, Nishida K, Miyazawa S, Komiyama T, Kadota Y, Abe N, Yoshida A, Hirohata S, Ohtsuka A and Ozaki T: Trichostatin A, a histone deacetylase inhibitor, suppresses synovial inflammation and subsequent cartilage destruction in a collagen antibody-induced arthritis mouse model. Osteoarthr Cartil (2008) 16: 723–732.

31. Iwamoto M, Hirohata S, Ogawa H, Ohtsuki T, Shinohata R, Miyoshi T, Hatipoglu FO, Kusachi S, Yamamoto K and Ninomiya Y: Connective tissue growth factor induction in a pressure-overloaded heart ameliorated by the angiotensin II type 1 receptor blocker olmesartan. Hypertens Res (2010) 33: 1305–1311.

32. Cilek MZ, Hirohata S, Faruk Hatipoglu O, Ogawa H, Miyoshi T, Inagaki J, Ohtsuki T, Harada H, Kamikawa S, Kusachi S, Ninomiya Y, Hatipoglu OF, Ogawa H, Miyoshi T and Inagaki J: AHR, a novel acute hypoxia-response sequence, drives reporter gene expression under hypoxia in vitro and in vivo. Cell Biol Int (2011) 35: 1–8.

33. Yamamoto K, Ohga N, Hida Y, Maishi N, Kawamoto T, Kitayama K, Akiyama K, Osawa T, Kondoh M, Matsuda K, Onodera Y, Fujie M, Kaga K, Hirano S, Shinohara N, Shindoh M and Hida K: Biglycan is a specific marker and an autocrine angiogenic factor of tumour endothelial cells. Br J Cancer (2012) 106: 1214–1223.

34. Obika M, Vernon RB, Gooden MD, Braun KR, Chan CK and Wight TN: ADAMTS-4 and Biglycan are Expressed at High Levels and Co-Localize to Podosomes During Endothelial Cell Tubulogenesis In Vitro. J Histochem Cytochem (2014) 62: 34–49.

35. Levicar N, Nutall RK and Lah TT: Proteases in brain tumour progression. Acta Neurochir (Wien) (2003) 145: 825–838.

36. Whellan DJ, Ellis SJ, Kraus WE, Hawthorne K, Piña IL, Keteyian SJ, Kitzman DW, Cooper L, Lee K and O'Connor CM: Method for establishing authorship in a multicenter clinical trial. Ann Intern Med (2009) 151: 414–420.

37. Fernández-Rodríguez R, Rodríguez-Baena FJ, Martino-Echarri E, Peris-Torres C, Plaza-Calonge M del C, Rodríguez-Manzaneque JC, Javier Rodríguez-Baena F, del Carmen Plaza-Calonge M, Carlos Rodríguez-Manzaneque J and María del Carmen Plaza-Calonge JCR-MRF-RFJR-BEM-ECP-T: Stroma-derived but not tumor ADAMTS1 is a main driver of tumor growth and metastasis. Oncotarget (2016) 7: 34507–34519.

38. Melching LI, Fisher WD, Lee ER, Mort JS and Roughley PJ: The cleavage of biglycan by aggrecanases. Osteoarthr Cartil (2006) 14: 1147–1154.

39. Li C, Xiong Y, Yang X, Wang L, Zhang S, Dai N, Li M, Ren T, Yang Y, Zhou SF, Gan L and Wang D: Lost expression of ADAMTS5 protein associates with progression and poor prognosis of hepatocellular carcinoma. Drug Des Devel Ther (2015) 9: 1773–1783.

40. Kumar S, Sharghi-Namini S, Rao N and Ge R: ADAMTS5 Functions as an Anti-Angiogenic and Anti-Tumorigenic Protein Independent of Its Proteoglycanase Activity. Am J Pathol (2012) 181: 1056–1068.